CHEMICAL ENGINEERING TRANSACTIONS
VOL. 62, 2017
A publication of AIDIC
The Italian Association of Chemical Engineering
Online at www.aidic.it/cet
Guest Editors: Fei Song,Haibo Wang, Fang He

ISBN978-88-95608- 60-0; **ISSN** 2283-9216
DOI: 10.3303/CET1762037

Methodology of Stoichiometry Based on Hyperspectral Image Recognition

Chengjia Yang*, Peng Tian, Chenghao Han

Jilin Jianzhu University, Changchun 130118, China
yang_chengjia@qq.com

This paper aims at researching a rapid, lossless, accurate and high-robustness classification model with the combination of hyperspectral image technology and stoichiometry to sole some problems in seed purity detection. The hyperspectral data is subject to the wave-band selection with the combination of stoichiometry, the mathematical model set up by using hyperspectral image is upgraded, and the seed purity is also tested. The experiment result indicates that: as the characteristic space of the original training set sample is enlarged by adding the new samples of 11.0%-12.8% of the predicted sample set in real time, the prediction accuracy of the upgraded model on the seed purity can be improved. Therefore, the online model upgrading strategy based on ISVDD can be used to improve the stability and generalization ability of the model well, and the requirements on instantaneity and accuracy of model upgrading in the actual production can be met.

1. Introduction

The hyperspectral image technology is the detecting technology widely used in the non-destructive measuring method of the farm product in recent years (Chen et al., 2014). Compared with the traditional machine vision and near-infrared spectrum analysis technique, the hyperspectral image technology can be used to obtain the image information such as the external shape and colour of the seed etc. simultaneously and reflect the spectral information of internal chemical component inside the seed (Chen et al., 2017), so that the multi-aspect and angle analysis on the tested object can be achieved. The hyperspectral image technology has been widely applied in the non-destructive measuring method of the farm product due to its advantages in many aspects. However, as the number of wave bands of the hyperspectral data is large (Chen et al., 2017), the data storage space is not only increased in the modelling analysis by using wave band, but also the actual calculation workload is increased, which can affect the real-time performance of the detection result. Actually (Dupré et al., 2017), high dependency and redundancy exist in adjacent wave bands of the hyperspectral image, due to which not every wave band is of the same value to the image processing (Elshamli et al., 2017). The least and most representative wave-band subsets are selected with wave-band selection algorithm to form the new hyperspectral image space, so that the original hyperspectral image space can be replaced approximately (He et al., 2017); thus, the dimensionality reduction of hyperspectral image data can be achieved, and the influence on the entire identification accuracy is smaller (Iordache et al., 2014), which is the final objective of hyperspectral-image waveband selection (Jia et al., 2017). Therefore, how to use the stoichiometry method to achieve the optimum wave-band selection is of importance value on rapid and accurate non-destructive testing of farm products (Kizel et al., 2017).

2. Hyperspectral image collection system

The near-infrared hyperspectral-image collection system (900-1700nm) is adopted in this experiment (Kumar S. and Singh S. K., 2017). The near-infrared hyperspectral-image collection system mainly consists of light source module, image collection module, sample delivery platform and the computer (Liao et al., 2016). The light source module is equipped with 150W fiber halogen lamp (2Specim, Spectral Imaging Ltd., Oulu, Finland), which can lead out the light source signal through two branches of optical fiber so as to form the eudipleural line source, and the light intensity is adjustable within the scope of 0-100% (Mei S, et al, 2017).

Please cite this article as: Chengjia Yang, Peng Tian, Chenghao Han, 2017, Methodology of stoichiometry based on hyperspectral image recognition, Chemical Engineering Transactions, 62, 217-222 DOI:10.3303/CET1762037

The image collection model mainly includes the N17E-QE line-scan imaging spectrometer (Spectral Imaging Ltd. Oulu, Finland) and the CCD camera with prismatic focusing magnifier. The spectrograph is the core part of the near-infrared hyperspectral-image collection system, the function of which is to resolve the complicated light into spectral lines (Moriya et al., 2017). Working principle: when on beam of composite light enters into the prism- raster- raster component, it will be gathered into the parallel light after entering into the entrance slit of the monochromator so as to be subject to chromatic dispersion through the diffraction grating based on different length of the beam wavelength (Mou and Ghamisi, 2017). The spectrum is formed through the focussing of focussing mirror based on the difference of angle in which each wave length leaving the optical grating finally (Mwaniki et al., 2015). The spectrum waveband scope covered by the line-scan imaging spectrometer is between 874-1734nm, and the spectral resolution is 5nm. The sample delivery platform is IRCP0076-type electric-control shift platform (Isuzu Optics Corp, Taiwan, China) (Ni and Ma, 2017). The resolution ratio of near-infrared hyperspectral image is 320*256 pixel (Papa et al., 2016). In case of near-infrared hyperspectral image collection, the parameters setting should be implemented through the collection software (Pardo et al., 2017). The image collection software of near-infrared hyperspectral imaging system is provided by Taiwan ISUZU Optics (Priebe et al., 2004). It is mainly used to control parameters collected by the image, including the moving speed of the platform and the exposure time of the camera etc (Rodriguez et al., 2017). The objective of image parameters adjustment is to obtain the clear, distortionless and sizeable hyperspectral image so as to make better preparation for the next experiment (Samek et al., 2017).

3. Hyperspectral image preprocessing

The image preprocessing is the operation of feature extraction and pre-modelling on the input image, and the main objective of which is to enhance the valuable information inside the image, and in the meanwhile, to restrain the information which may cause unnecessary interference on the feature extraction and data modelling later in the image (Selvam and Karuppiah, 2017). The final objective of the preprocessing in the experiment is to obtain the external profile information of the seed; however, hyperspectral image is the three-dimensional information containing the two-dimensional image information and one-dimensional waveband information (Tan et al., 2017); the profile information of the seed corresponding to each waveband is unique. In order to avoid the complexity of the experiment operation, the ENVI4.3 software is used in the experiment to select the image showing the clear profile of corn seed in a waveband for the preprocessing operation; finally, the profile extracted will be mapped to all wavebands so as to extract the spectral information of all wavebands of the seed. See the preprocessing operation procedures in the Figure 1.

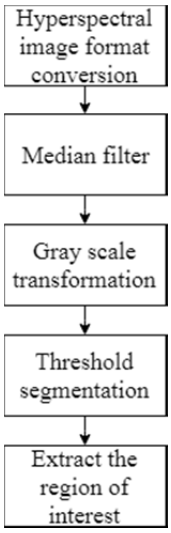

Figure 1: Preprocessing Operation of Hyperspectral Image Identification of the Seed

4. Technical route for hyperspectral image identification of the seed

See the technical route of hyperspectral image identification system of the seed in Figure 2, which includes the collection of hyperspectral images, correction and preprocessing of images, image division and feature extraction (Wang et al., 2017); the prediction is implemented to the samples to be tested by modelling and using the well-trained models so as to achieve the seed purity identification (Xia et al., 2016).

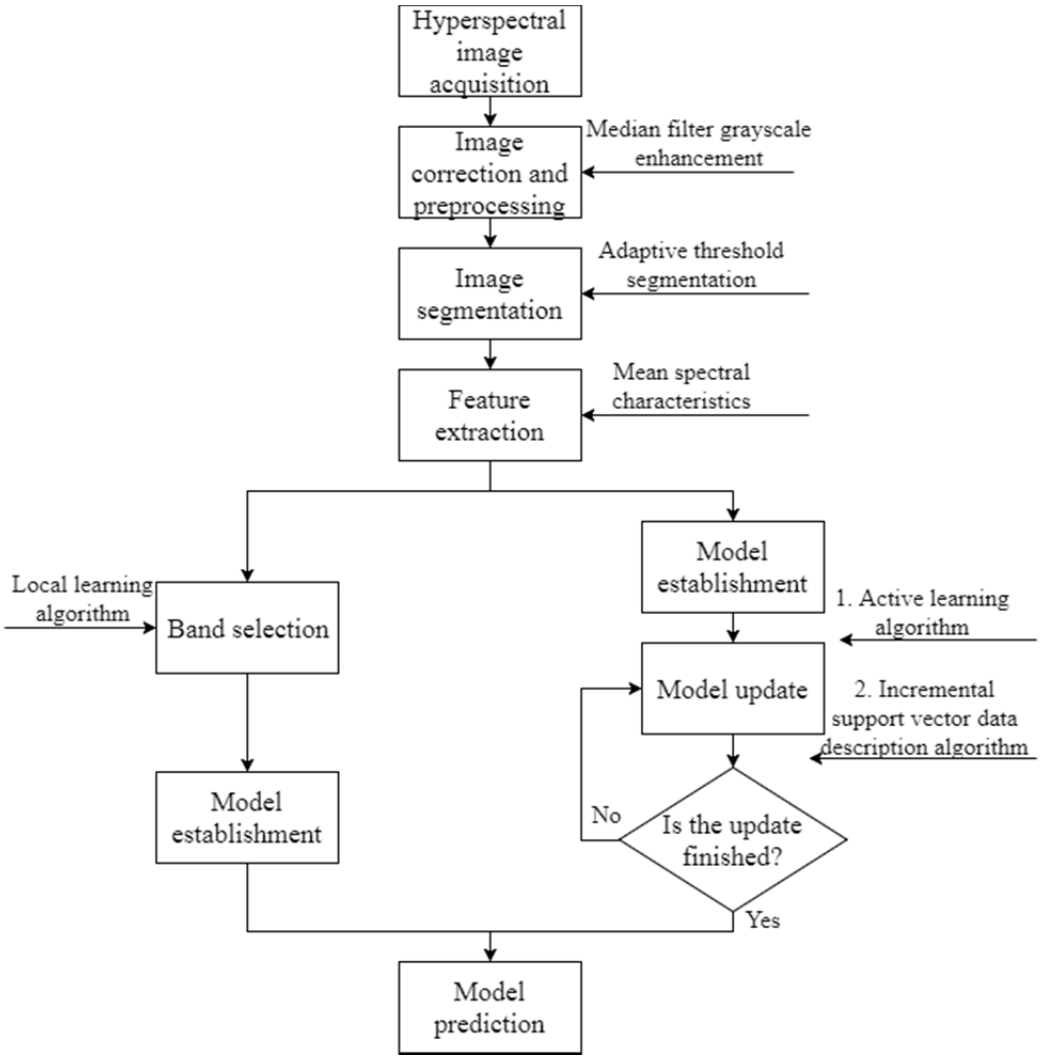

Figure 2: Technical Route of Hyperspectral Image Identification of the Seed

5. Experiment result and analysis

5.1 Establishment of core-seed purity detection model

In order to eliminate the influence of overlarge difference among characteristic parameters of different wavebands on the modelling result, the characteristic parameters are subject to the normalization processing before modelling of corn-seed purity detection. Then two groups of experiment are designed for the data after normalization processing, which is the corn-seed purity detection models of 2010 and 2011. Firstly, the Kennard-Stone algorithm (KS) is used to divide the XY2010 and ZD2010 of corn seed of the year 2011 into the training set and the test set based on different proportions (1:1, 3:1 and 4:1), and the SVM category-prediction model M2010 is set up so as to obtain the training accuracy cR and prediction accuracy P1R (Yang W, et al, 2017). Then the SVM category-prediction model M2011 of corn seed of year 2011 is set up with the same method. At last, in order to inspect the suitability of the model to samples of other years, the M2010 is used to predict 400 corn seeds of year 2011 and M2011 is used to predict 240 corn seeds of year 2010 directly and separately, the prediction accuracy of which is RP2; see the corn-seed purity detection model result in the Table 1.

According to this table, the prediction accuracy of M2010 and M2011 on the corn seed of the same year reaches 100%; however, according to the suitability detection of the new sample, the prediction accuracy of corn seeds of other years can only reach 33.8%~54.6%, which further indicates that the spectral information can be easily affected by years, thus the stability of model established with spectral information is obviously affected by changes in years of the corn seeds; the universal performance of models established in different years is poor.

Table 1: Result of Corn-seed Purity Detection Model (%)

Division ratio	M_{2010}			M_{2011}		
	R_c	R_{P1}	R_{P2}	R_c	R_{P1}	R_{P2}
1:1	100	100	47.0	100	100	50.8
3:1	100	100	33.8	99.7	100	54.6
4:1	100	100	49.0	100	100	53.8

Table 2: Prediction Accuracy Comparison of New Samples Before and After the Upgrading of Corn-seed Purity Detection Model (%)

Division ratio	M_{2010}		M_{2011}	
	Before updating	After updating (40)	Before updating	After updating (56)
1:1	47.0	98.9	50.8	94.6
3:1	33.8	98.3	54.6	94.0
4:1	49.0	98.3	53.8	94.6

As shown in Table 2 and under the division proportion of three different sample sets, in case 40 new samples are added by using active learning are used to achieve the upgrading of the 2010 model, the prediction accuracy on new samples can reach 98.9%, 98.3% and 98.3% separately; in case 56 new samples are added by using active learning to achieve the upgrade of 2011 model, the prediction accuracy on new samples can also reach 94.6%, 94% and 94.6% separately. No matter the year2010 or the year 2011, the model upgraded based on active-learning algorithm is obviously improved compared with the prediction accuracy of new sample before the upgrading; what's more, the upgrading effect and the division proportion of old sample model is nearly subject to no relationship, the better stability can be achieved. The model classification result analysis of ISVDD-based online upgrading strategy is similar to the model before upgrading; in consideration of the effect of randomness in sample division on the experiment result, random 5 times are divided in the training set (800*94) and the prediction set (1200*94). In addition, as the sequence of learning one-by-one of prediction sample may affect the upgrading quality of the model, 4 times experiments are also implemented to the prediction set (1200*94) randomly which is divided randomly each time. The final experiment result is subject to the average result of 20 random times as the classification accuracy of LSSVN after the upgrading. The average classification result of the upgraded LSSVM model is shown in Table 3. See the number of samples rejected in identification during random 20 times in Table 4 (s means the random times of the division of training set and prediction set; t means the number of times of self-random for prediction set).

Table 3: Average Classification Result of the Upgraded LSSVM Model (%)

Type	Training accuracy	Prediction accuracy
JIDAN7	100	99.4
JUNDAN18	100	93.0
JUNDAN20	100	87.7
LUDAN818	100	97.4
Average classification accuracy	100	94.4

Table 4: Number of Samples Rejected in Identification during the Upgrading Process

Times	1t	2t	3t	4t
1s	133	142	145	147
2s	136	153	137	143
3s	138	143	140	143
4s	132	140	135	141
5s	133	142	139	143

According to Table 3, except for JIDAN7, the JUNDAN18, JUNDAN20 and LUDAN818 prediction accuracy is obviously improved in the comparison with that before the upgrading, which is improved by 23.7%, 10.2% and

7% separately. The average classification accuracy of the entire classification model also reaches 94.4%, which is improved by 10.3% against the 84.1% before upgrading. According to Table 4, the upgrading of the model is only achieved by adding the 11.0%-12.8% new samples to the original training samples, the influence of learning sequence before and after the prediction set sample is not obvious.

6. Conclusion

The spectral features of the seed can be changed under the influence of years, which results in obvious differences of the spectral features of seeds in the same category but different years. The model upgrading can be hardly subject to the complete training set sample during the actual production process, which results in the stability and generalization ability reduction of the model. To solve this problem, the new strategy of ISVDD-based online model upgrading can be effectively applied to improve the stability and generalization ability of the mode, and can meet the requirements on instantaneity and accuracy of model upgrading in the actual production.

Reference

Chen G., Li C., Sun W., 2017, Hyperspectral face recognition via feature extraction and CRC-based classifier, IET Image Processing, 11, 266-272, DOI: 10.1049/iet-ipr.2016.0722

Chen G., Sun W., Xie W., 2017, Hyperspectral face recognition with log-polar Fourier features and collaborative representation based voting classifiers, IET Biometrics, 6, 36-42, DOI: 10.1049/iet-bmt.2015.0103

Chen T., Yuen P., Richardson M., Liu G., She Z., 2014, Detection of Psychological Stress Using a Hyperspectral Imaging Technique, IEEE Transactions on Affective Computing, 5, 391-405, DOI: 10.1109/TAFFC.2014.2362513

Dupré A., Ricciardi G., Bourennane S., Mylvaganam S., 2017, Electrical Capacitance-Based Flow Regimes Identification ---Multiphase Experiments and Sensor Modeling, IEEE Sensors Journal, 17, 8117-8128, DOI: 10.1109/JSEN.2017.2707659

Elshamli A., Taylor G. W., Berg A., Areibi S., 2017, Domain Adaptation Using Representation Learning for the Classification of Remote Sensing Images, IEEE Journal of Selected Topics in Applied Earth Observations and Remote Sensing, 10, 4198-4209, DOI: 10.1109/JSTARS.2017.2711360

He L., Li J., Liu C., Li S., 2017, Recent Advances on Spectral-Spatial Hyperspectral Image Classification: An Overview and New Guidelines, IEEE Transactions on Geoscience and Remote Sensing, 1-19, DOI: 10.1109/TGRS.2017.2765364

Iordache M. D., Tits L., Bioucas-Dias J. M., Plaza A., Somers B., 2014, A Dynamic Unmixing Framework for Plant Production System Monitoring, IEEE Journal of Selected Topics in Applied Earth Observations and Remote Sensing, 7, 2016-2034, DOI: 10.1109/JSTARS.2014.2314960

Jia S., Shen L., Zhu J., Li Q., 2017, A 3-D Gabor Phase-Based Coding and Matching Framework for Hyperspectral Imagery Classification, IEEE Transactions on Cybernetics, 1-13, DOI: 10.1109/TCYB.2017.2682846

Kizel F., Shoshany M., Netanyahu N. S., Even-Tzur G., Benediktsson J. A., 2017, A Stepwise Analytical Projected Gradient Descent Search for Hyperspectral Unmixing and Its Code Vectorization, IEEE Transactions on Geoscience and Remote Sensing, 55, 4925-4943, DOI: 10.1109/TGRS.2017.2692999

Kumar S., Singh S. K., 2017, Visual animal biometrics: survey, IET Biometrics, 6, 139-156, DOI: 10.1049/iet-bmt.2016.0017

Liao W., Mura M. D., Chanussot J., Pižurica A., 2016, Fusion of Spectral and Spatial Information for Classification of Hyperspectral Remote-Sensed Imagery by Local Graph, IEEE Journal of Selected Topics in Applied Earth Observations and Remote Sensing, 9, 583-594, DOI: 10.1109/JSTARS.2015.2498664

Mei S., Ji J., Hou J., Li X., Du Q., 2017, Learning Sensor-Specific Spatial-Spectral Features of Hyperspectral Images via Convolutional Neural Networks, IEEE Transactions on Geoscience and Remote Sensing, 55, 4520-4533, DOI: 10.1109/TGRS.2017.2693346

Moriya É. A. S., Imai N. N., Tommaselli A. M. G., Miyoshi G. T., 2017, Mapping Mosaic Virus in Sugarcane Based on Hyperspectral Images, IEEE Journal of Selected Topics in Applied Earth Observations and Remote Sensing, 10, 740-748, DOI: 10.1109/JSTARS.2016.2635482

Mou L., Ghamisi P., Zhu X. X., 2017, Deep Recurrent Neural Networks for Hyperspectral Image Classification, IEEE Transactions on Geoscience and Remote Sensing, 55, 3639-3655, DOI: 10.1109/TGRS.2016.2636241

Mwaniki M. W., Matthias M. S., Schellmann G., 2015, Application of Remote Sensing Technologies to Map the Structural Geology of Central Region of Kenya, IEEE Journal of Selected Topics in Applied Earth Observations and Remote Sensing, 8, 1855-1867, DOI: 10.1109/JSTARS.2015.2395094

Ni D., Ma H., 2017, Fast Classification of Hyperspectral Images Using Globally Regularized Archetypal Representation With Approximate Solution, IEEE Transactions on Geoscience and Remote Sensing, 55, 2414-2430, DOI: 10.1109/TGRS.2016.2643166

Papa J. P., Papa L. P., Pereira D. R., Pisani R. J., 2016, A Hyperheuristic Approach for Unsupervised Land-Cover Classification, IEEE Journal of Selected Topics in Applied Earth Observations and Remote Sensing, 9, 2333-2342, DOI: 10.1109/JSTARS.2016.2557584

Pardo A., Real E., Krishnaswamy V., López-Higuera J. M., Pogue B. W., Conde O. M., 2017, Directional Kernel Density Estimation for Classification of Breast Tissue Spectra, IEEE Transactions on Medical Imaging, 36, 64-73, DOI: 10.1109/TMI.2016.2593948

Priebe C. E., Marchette D. J., Healy D. M., 2004, Integrated sensing and processing decision trees, IEEE Transactions on Pattern Analysis and Machine Intelligence, 26, 699-708, DOI: 10.1109/TPAMI.2004.12

Rodriguez P., Cucurull G., Gonzàlez J., Gonfaus J. M., Nasrollahi K., Moeslund T. B., Roca F. X., 2017, Deep Pain: Exploiting Long Short-Term Memory Networks for Facial Expression Classification, IEEE Transactions on Cybernetics, 1-11, DOI: 10.1109/TCYB.2017.2662199

Samek W., Binder A., Montavon G., Lapuschkin S., Müller K. R., 2017, Evaluating the Visualization of What a Deep Neural Network Has Learned, IEEE Transactions on Neural Networks and Learning Systems, 28, 2660-2673, DOI: 10.1109/TNNLS.2016.2599820

Selvam I.R. P., Karuppiah M., 2017, Gender recognition based on face image using reinforced local binary patterns, IET Computer Vision, 11, 415-425, DOI: 10.1049/iet-cvi.2016.0087

Tan J., Zhang J., Zhang Y., 2017, Target Detection for Polarized Hyperspectral Images Based on Tensor Decomposition, IEEE Geoscience and Remote Sensing Letters, 14, 674-678, DOI: 10.1109/LGRS.2017.2671439

Wang Z., Du B., Zhang L., Zhang L., Jia X., 2017, A Novel Semisupervised Active-Learning Algorithm for Hyperspectral Image Classification, IEEE Transactions on Geoscience and Remote Sensing, 55, 3071-3083, DOI: 10.1109/TGRS.2017.2650938

Xia J., Falco N., Benediktsson J. A., Chanussot J., Du P., 2016, Class-Separation-Based Rotation Forest for Hyperspectral Image Classification, IEEE Geoscience and Remote Sensing Letters, 13, 584-588, DOI: 10.1109/LGRS.2016.2528043

Yang W., Hou K., Liu B., Yu F., Lin L., 2017, Two-Stage Clustering Technique Based on the Neighboring Union Histogram for Hyperspectral Remote Sensing Images, IEEE Access, 5, 5640-5647, DOI: 10.1109/ACCESS.2017.2695616